A mechanistic model of connector hubs, modularity, and cognition

Maxwell A. Bertolero[1,2*], B.T. Thomas Yeo[3,4], Danielle S. Bassett[2,5-7], Mark D'Esposito[1]

[1]Helen Wills Neuroscience Institute and the Department of Psychology, University of California, Berkeley, CA 94720-3190, USA
[2]Department of Bioengineering, School of Engineering and Applied Sciences, University of Pennsylvania, Philadelphia, PA 19104 USA
[3]Electrical and Computer Engineering, ASTAR-NUS Clinical Imaging Research Centre, Singapore Institute for Neurotechnology & Memory Networks Programme, National University of Singapore, Singapore 119077, Singapore
[4]NUS Graduate School for Integrative Sciences and Engineering, National University of Singapore, Singapore
[5]Department of Electrical & Systems Engineering, School of Engineering and Applied Sciences, University of Pennsylvania, Philadelphia, PA 19104, USA
[6]Department of Physics & Astronomy, College of Arts and Sciences, University of Pennsylvania, Philadelphia, PA 19104 USA
[7]Department of Neurology, Perelman School of Medicine, University of Pennsylvania, Philadelphia, PA 19104 USA.
*corresponding author (mbertolero@me.com)

Supplementary Information

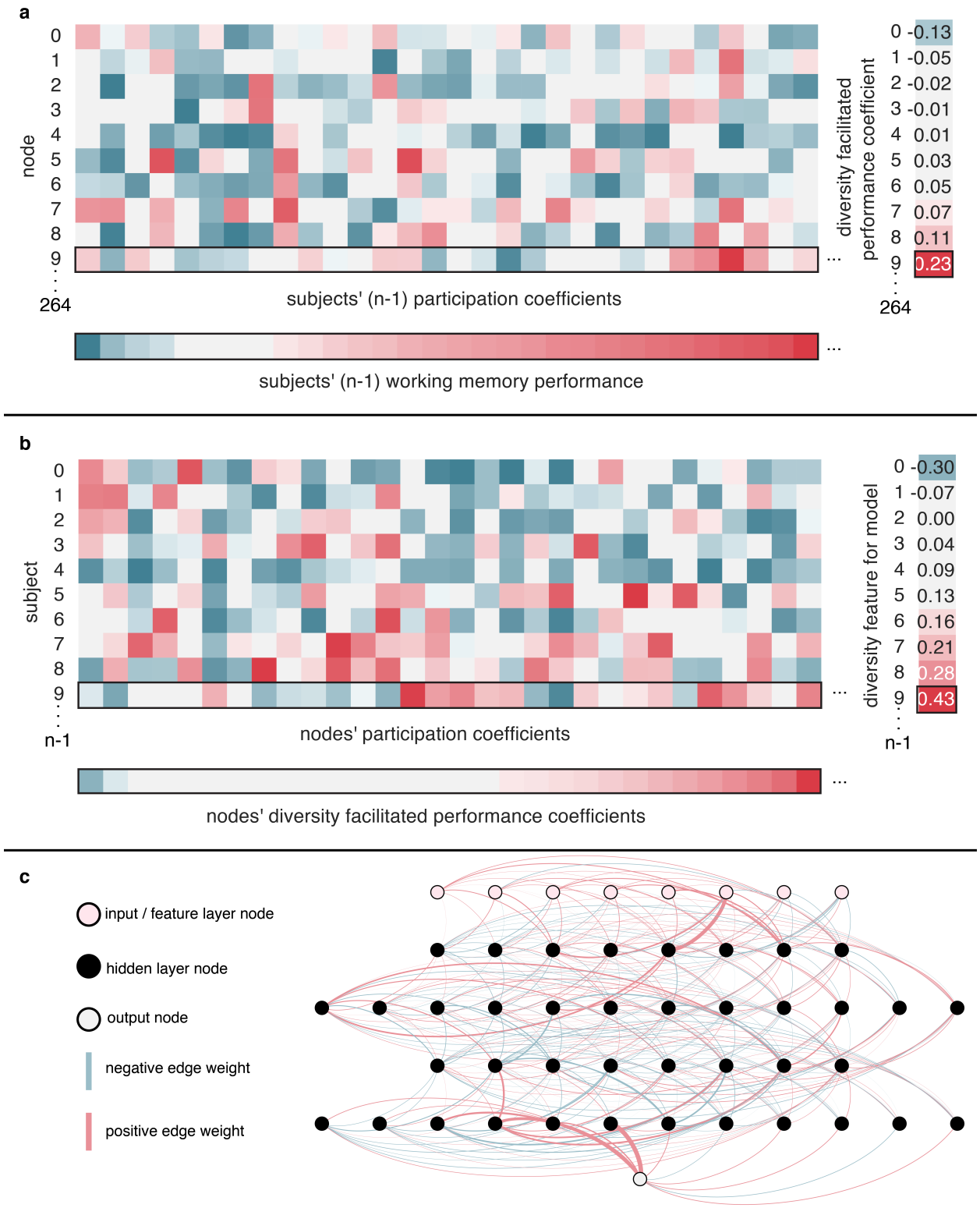

Supplementary Figure 1. **Workflow of the deep neural network features and model construction. a**, For each node, we measured the diversity facilitated performance coefficient. For example, the Pearson *r* is calculated between node 9's participation coefficients across subjects (black outline) and task performance across subjects (black outline), resulting in a diversity facilitated performance coefficient of 0.23 (black outline) for that node. **b**, The optimality of a subject's participation coefficients for task performance is measured by, for example, calculating the Pearson *r* between subject 9's participation coefficients (black outline) and the diversity facilitated performance coefficients (black outline), resulting in a diversity feature for the model of 0.43 (black outline).

The same procedures in **a** and **b** are also executed using within community strengths and edge weights instead of participation coefficients. Modularity (Q) values are also used as features. These four features are derived separately from resting-state and the task network for which task performance is being predicted, resulting in eight features. All calculations in panels **a** and **b** are calculated without data from the subject for which the prediction is being made. These eight features are then used in a deep neural network model (**c**) to learn the relationship between the features and task performance (again, without data from the subject for which the prediction is being made) by adjusting the weights between nodes in adjacent layers. The features are then calculated for the left-out subject (e.g., Pearson *r* between the left-out subject's participation coefficients and the previously calculated diversity facilitated performance coefficients that did not include data from the left-out subject) and are used in the deep neural network model to generate a prediction for the left-out subject.

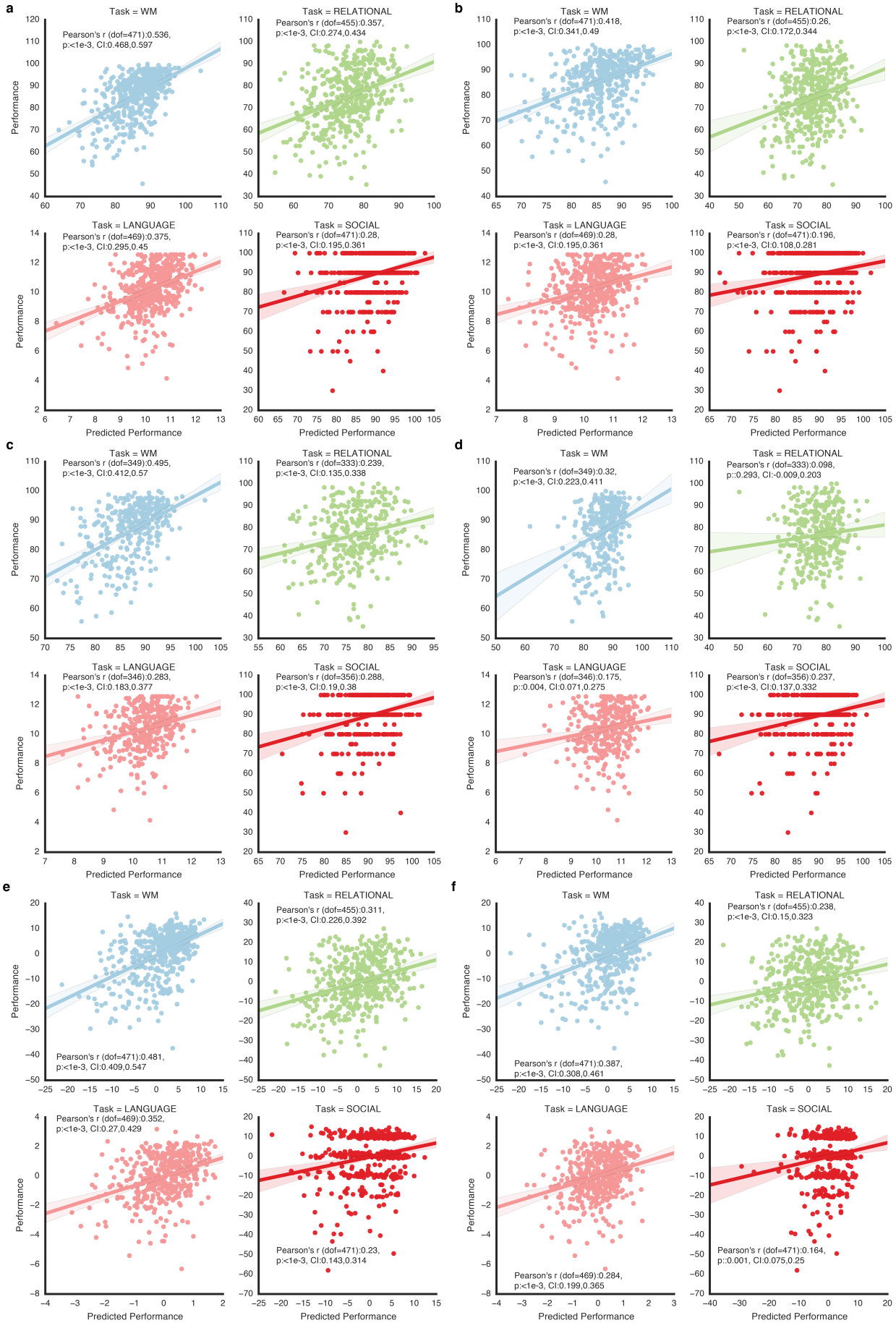
a
Task = WM
Pearson's r (dof=471):0.536,
p:<1e-3, CI:0.468,0.597
Task = RELATIONAL
Pearson's r (dof=455):0.357,
p:<1e-3, CI:0.274,0.434
Task = LANGUAGE
Pearson's r (dof=469):0.375,
p:<1e-3, CI:0.295,0.45
Task = SOCIAL
Pearson's r (dof=471):0.28,
p:<1e-3, CI:0.195,0.361
b
Task = WM
Pearson's r (dof=471):0.418,
p:<1e-3, CI:0.341,0.49
Task = RELATIONAL
Pearson's r (dof=455):0.26,
p:<1e-3, CI:0.172,0.344
Task = LANGUAGE
Pearson's r (dof=469):0.28,
p:<1e-3, CI:0.195,0.361
Task = SOCIAL
Pearson's r (dof=471):0.196,
p:<1e-3, CI:0.108,0.281
c
Task = WM
Pearson's r (dof=349):0.495,
p:<1e-3, CI:0.412,0.57
Task = RELATIONAL
Pearson's r (dof=333):0.239,
p:<1e-3, CI:0.135,0.338
Task = LANGUAGE
Pearson's r (dof=346):0.283,
p:<1e-3, CI:0.183,0.377
Task = SOCIAL
Pearson's r (dof=356):0.288,
p:<1e-3, CI:0.19,0.38
d
Task = WM
Pearson's r (dof=349):0.32,
p:<1e-3, CI:0.223,0.411
Task = RELATIONAL
Pearson's r (dof=333):0.098,
p::0.293, CI:-0.009,0.203
Task = LANGUAGE
Pearson's r (dof=346):0.175,
p::0.004, CI:0.071,0.275
Task = SOCIAL
Pearson's r (dof=356):0.237,
p:<1e-3, CI:0.137,0.332
e
Task = WM
Pearson's r (dof=471):0.481,
p:<1e-3, CI:0.409,0.547
Task = RELATIONAL
Pearson's r (dof=455):0.311,
p:<1e-3, CI:0.226,0.392
Task = LANGUAGE
Pearson's r (dof=469):0.352,
p:<1e-3, CI:0.27,0.429
Task = SOCIAL
Pearson's r (dof=471):0.23,
p:<1e-3, CI:0.143,0.314
f
Task = WM
Pearson's r (dof=471):0.387,
p:<1e-3, CI:0.308,0.461
Task = RELATIONAL
Pearson's r (dof=455):0.238,
p:<1e-3, CI:0.15,0.323
Task = LANGUAGE
Pearson's r (dof=469):0.284,
p:<1e-3, CI:0.199,0.365
Task = SOCIAL
Pearson's r (dof=471):0.164,
p::0.001, CI:0.075,0.25
Performance
Predicted Performance

Supplementary Figure 2 | **Hub diversity and locality, modularity, and network connectivity predicts task performance**. **a**, predictive model of task performance (see Methods for performance measures), as shown in Figure 2a. **b**, Predictive model of task performance without using network connectivity (i.e., only hub diversity and locality and modularity). *N*=Working Memory: 473, Relational: 457,Language & Math: 471, Social: 473). Each dot represents a subject's prediction. Shaded areas represent 95 percent confidence intervals. **c**,**d**, As in **a**,**b**, except the frames with high motion were removed from the time series before the network of that individual was constructed (i.e., scrubbing), *N*=Working Memory: 351, Relational: 335, Language & Math: 348, Social: 358, as subjects with less than 75 percent of frames after scrubbing were not analyzed. **e**,**f**, As in **a**,**b**, except mean frame wise displacement was regressed out from the task performance values, *N*=Working Memory: 473, Relational: 457,Language & Math: 471, Social: 473). All *p* values are Bonferroni corrected (*n* tests=4).

Supplementary Figure 3. **Feature correspondence between tasks and subject measures**. To test if certain hub and network structures that are optimal to each task (Language & Math, Relational, Social, or Working Memory) are also optimal for other subject measures, we measured the feature correspondence between subjects' features in the task model with the subjects' features in the same model that was fit to a given subject measure (e.g., Delayed Discounting) instead of performance in the task. The feature correspondence is shown for each task; high feature correspondence means a similar hub and network structure is optimal for the task and subject measure. Colors represent z-scored (within column) feature correspondence values. Results significant at $p<1\text{-}e3$ uncorrected, $p<0.05$ Bonferroni corrected (*N* tests= 47) are marked with an asterisk. *N* subjects = Working Memory: 473, Relational: 457,Language & Math: 471, Social: 473).

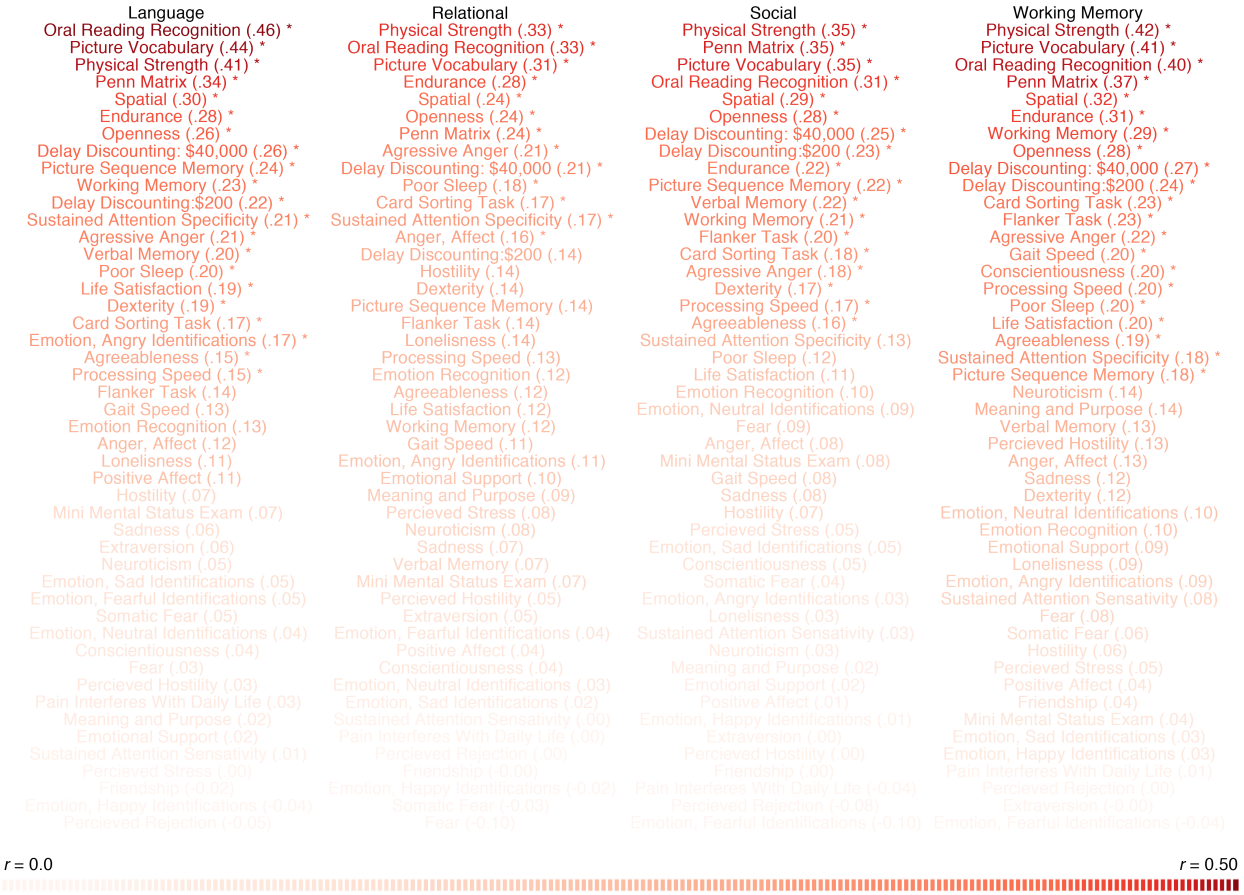

Supplementary Figure 4 | **Prediction of subject measures by the model of hub diversity and locality, modularity, and network connectivity**. As in Figure 1, we predicted each subject measure using a model of hub diversity and locality, modularity, and network connectivity. This was executed for networks constructed based on the data from each task (columns). For each task and subject measure, the Pearson *r* between the real subject measure values and the predicted subject measure values are shown. Colors represent the *z*-scored (within each task) Pearson *r*. Predictions that are significant ($p<1\text{-e}3$ uncorrected, $p<0.05$ after Bonferroni correction, *N* tests = 47) are marked with an asterisk. *N*= Working Memory: 473, Relational: 457, Language & Math: 471, Social: 473).

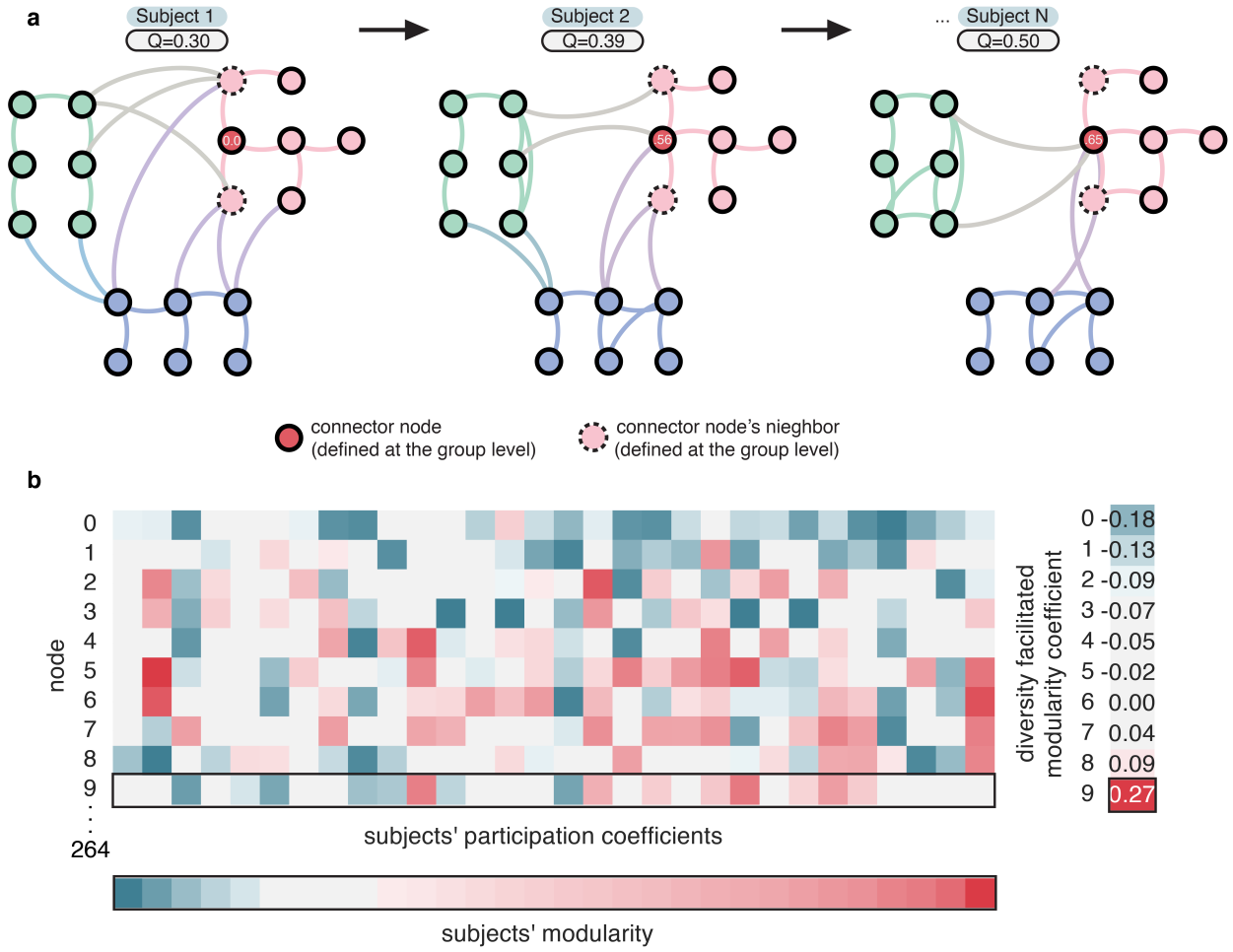

Supplementary Figure 5 | **Analyzing individual differences of hubs' diversity and locality and modularity**. When connector hubs are connected to many communities (as indicated by high participation coefficients), they can integrate information and tune connectivity optimally, allowing other regions to perform more modular local processing. Thus, across subjects, we predicted that the increased participation coefficients (i.e., diversity) of connector hubs would be correlated with preservations or increases in the modularity (*Q*) of the network. This prediction is illustrated above (**a**). Each graph represents the network structure of an individual subject. A single connector hub, shown in red, is identified based on its high mean participation coefficient across individuals; subject-level participation coefficient values are shown inside the red nodes. Local neighborhoods or *communities* are shown in green, blue, and pink, and subject-level values of modularity(*Q*) are shown above each graph. Across subjects, we predict that higher participation coefficients of connector hubs will occur in more modular networks in which the neighbors of connector hubs (pink, dashed-outline) display more local connectivity. **b**, To test this prediction, for each node we measured the diversity facilitated modularity coefficient; for example, the Pearson *r* is calculated between node 9's participation coefficients across subjects (black outline) and modularity (*Q*) across subjects (black outline), resulting in a diversity facilitated modularity coefficient of 0.27 (black outline).

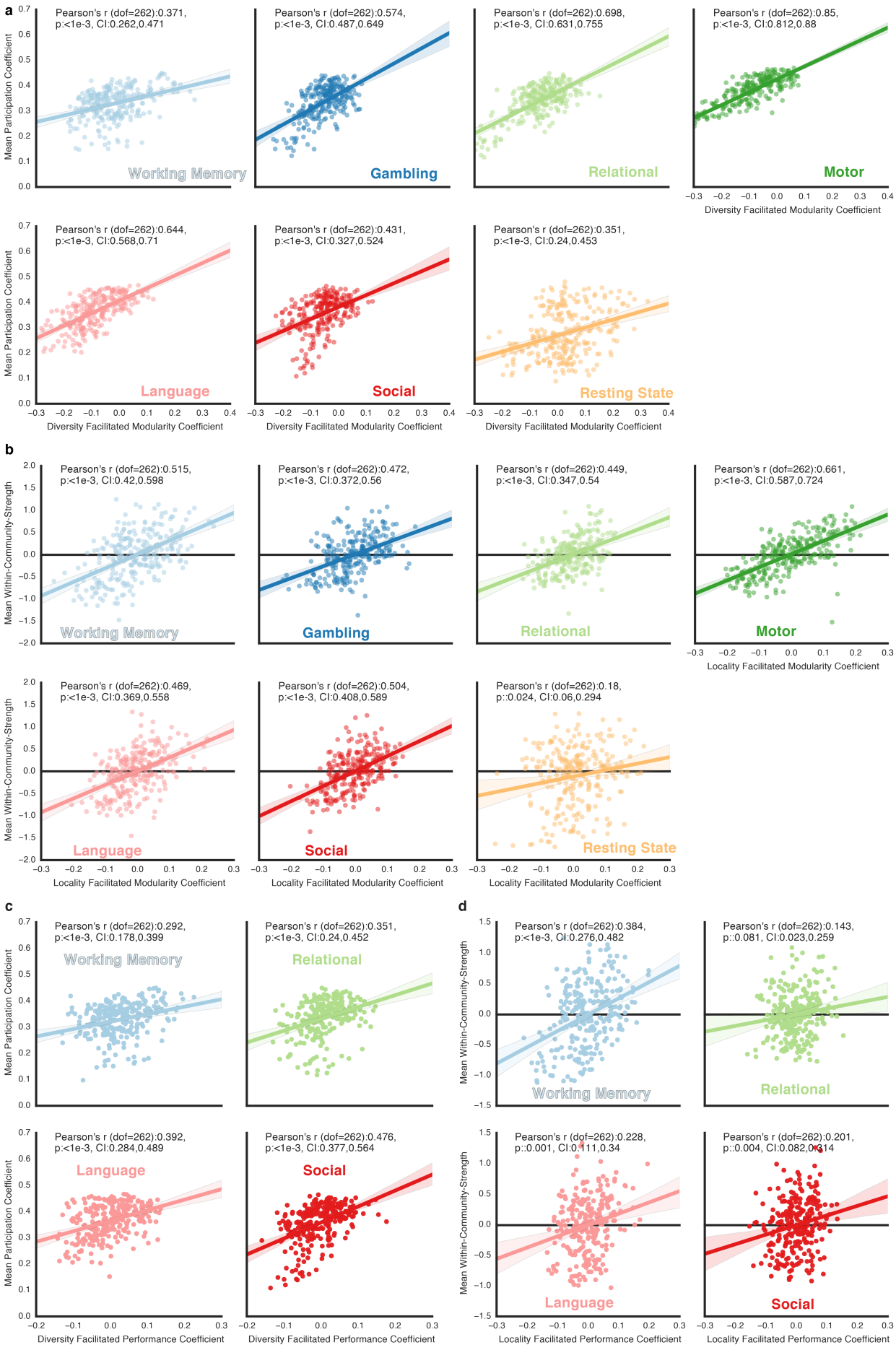
a
Pearson's r (dof=262):0.371, p:<1e-3, CI:0.262,0.471
Working Memory
Pearson's r (dof=262):0.574, p:<1e-3, CI:0.487,0.649
Gambling
Pearson's r (dof=262):0.698, p:<1e-3, CI:0.631,0.755
Relational
Pearson's r (dof=262):0.85, p:<1e-3, CI:0.812,0.88
Motor
Mean Participation Coefficient
Diversity Facilitated Modularity Coefficient
Pearson's r (dof=262):0.644, p:<1e-3, CI:0.568,0.71
Language
Pearson's r (dof=262):0.431, p:<1e-3, CI:0.327,0.524
Social
Pearson's r (dof=262):0.351, p:<1e-3, CI:0.24,0.453
Resting State
b
Pearson's r (dof=262):0.515, p:<1e-3, CI:0.42,0.598
Working Memory
Pearson's r (dof=262):0.472, p:<1e-3, CI:0.372,0.56
Gambling
Pearson's r (dof=262):0.449, p:<1e-3, CI:0.347,0.54
Relational
Pearson's r (dof=262):0.661, p:<1e-3, CI:0.587,0.724
Motor
Mean Within-Community-Strength
Locality Facilitated Modularity Coefficient
Pearson's r (dof=262):0.469, p:<1e-3, CI:0.369,0.558
Language
Pearson's r (dof=262):0.504, p:<1e-3, CI:0.408,0.589
Social
Pearson's r (dof=262):0.18, p::0.024, CI:0.06,0.294
Resting State
c
Pearson's r (dof=262):0.292, p:<1e-3, CI:0.178,0.399
Working Memory
Pearson's r (dof=262):0.351, p:<1e-3, CI:0.24,0.452
Relational
Mean Participation Coefficient
Diversity Facilitated Performance Coefficient
Pearson's r (dof=262):0.392, p:<1e-3, CI:0.284,0.489
Language
Pearson's r (dof=262):0.476, p:<1e-3, CI:0.377,0.564
Social
d
Pearson's r (dof=262):0.384, p:<1e-3, CI:0.276,0.482
Working Memory
Pearson's r (dof=262):0.143, p::0.081, CI:0.023,0.259
Relational
Mean Within-Community-Strength
Locality Facilitated Performance Coefficient
Pearson's r (dof=262):0.228, p::0.001, CI:0.111,0.34
Language
Pearson's r (dof=262):0.201, p::0.004, CI:0.082,0.314
Social

Supplementary Figure 6 | **Connector and local hubs facilitate network modularity and task performance**. **a**, correlations between a node's mean participation coefficient (across subjects) and the node's diversity facilitated modularity coefficient (the Pearson *r* correlation coefficient between that node's participation coefficients and modularity values (*Q*) across subjects). Correlations were calculated for each cognitive state. Each dot represents a node in the brain's functional network. Shaded areas represent 95 percent confidence intervals. In all cognitive states, there was a significant positive correlation between a node's mean participation coefficient and the node's diversity facilitated modularity coefficient. This demonstrates that connector hubs facilitate increased modularity. **b**, correlations between a node's mean within community strength (across subjects) and the node's locality facilitated modularity coefficient (Pearson *r* correlation coefficient between that node's within community strengths and modularity values (*Q*) across subjects). In all cognitive states, there was a significant positive correlation between a node's within community strength and the node's locality facilitated modularity coefficient. This demonstrates that local hubs facilitate increased modularity. **c**, correlations between a node's mean participation coefficient (across subjects) and the node's diversity facilitated performance coefficient (the Pearson *r* correlation coefficient between that node's participation coefficients and task performance across subjects). Correlations were calculated for each cognitive state. Each dot represents a node in the brain's functional network. Shaded areas represent 95 percent confidence intervals. In all cognitive states, there was a significant positive correlation between a node's mean participation coefficient and the node's diversity-facilitated performance coefficient. This demonstrates that connector hubs facilitate increased task performance. **d**, correlations between a node's mean within community strength (across subjects) and the node's locality facilitated performance coefficient (Pearson *r* correlation coefficient between that node's within community strengths and task performance across subjects). In all cognitive states (except Relational, Bonferroni (*n* tests=4) p=0.081, uncorrected p=0.02), there was a significant positive correlation between a node's within community strength and the node's locality facilitated performance coefficient. Bonferroni corrected *p* values are shown (*n* tests=7(a,b), and 4(c,d). N=264, the number of nodes in the graph. This demonstrates that local hubs facilitate increased task performance.

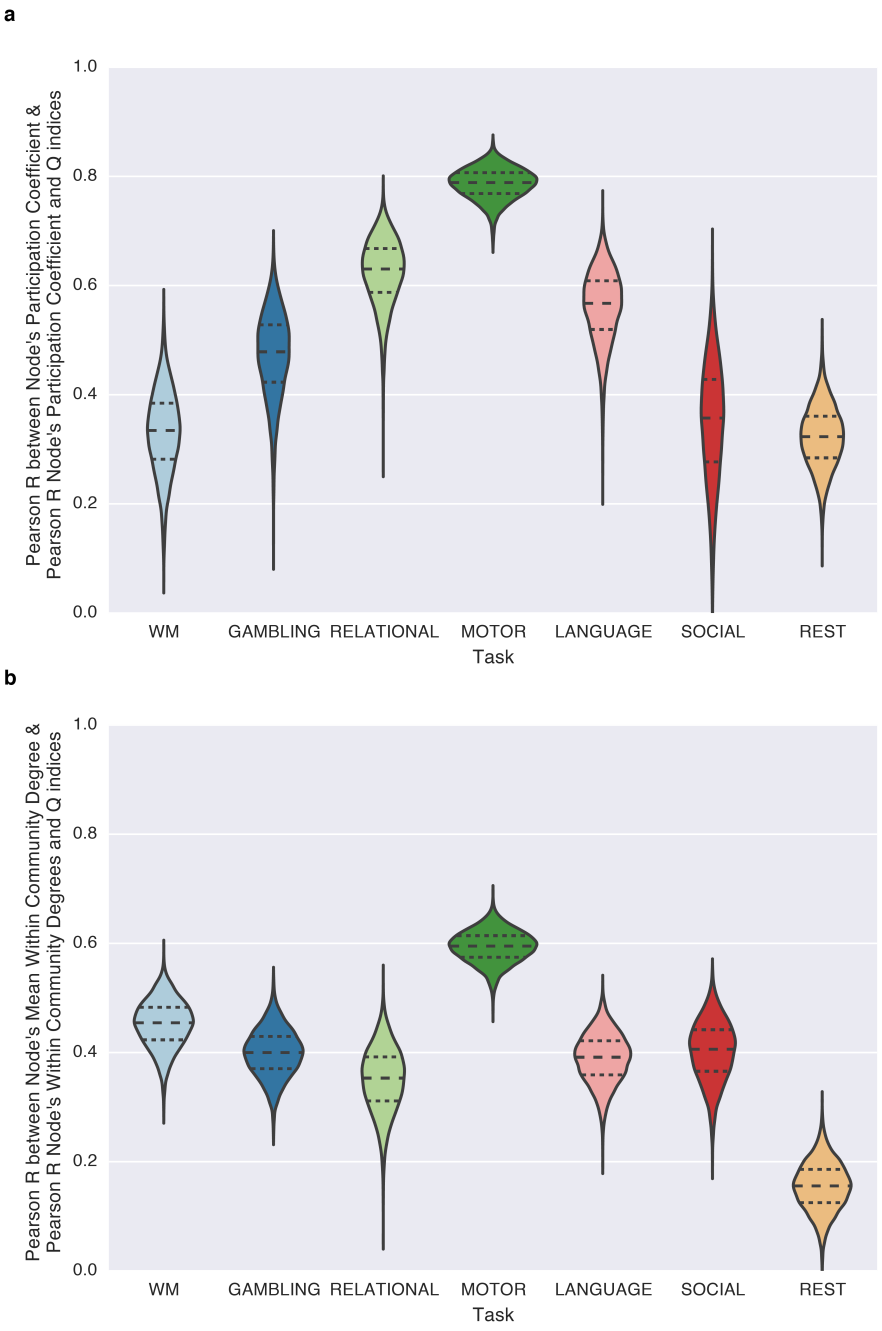

Supplementary Figure 7 | **Cross validation of diversity and locality facilitated modularity coefficients**. Connector hubs and local hubs are defined by a higher participation coefficient and within community strength, respectively, across subjects on average. To avoid potential dependencies, we estimated the mean within community strength or participation coefficient of each node in one half of subjects, and the correlation between a nodes' within community strength or participation coefficients and *Q* indices—the node's locality and diversity facilitated modularity coefficients—in the other half, testing 10,000 split of subjects. On average, correlations were still significant in every state. **a**, The distribution of Pearson *r* values between a node's mean participation coefficient (defined in half the subjects) and the diversity facilitated modularity coefficient (defined in the other half of the subjects). **b**, The distribution of Pearson *r* values between a node's mean within community strength (defined in half the subjects) and the locality facilitated modularity coefficient (defined in the other half of the subjects). *N*=264, the number of nodes in the graph, for each *r* value calculation, (dof=262). The mean and quartiles are marked in each violin.

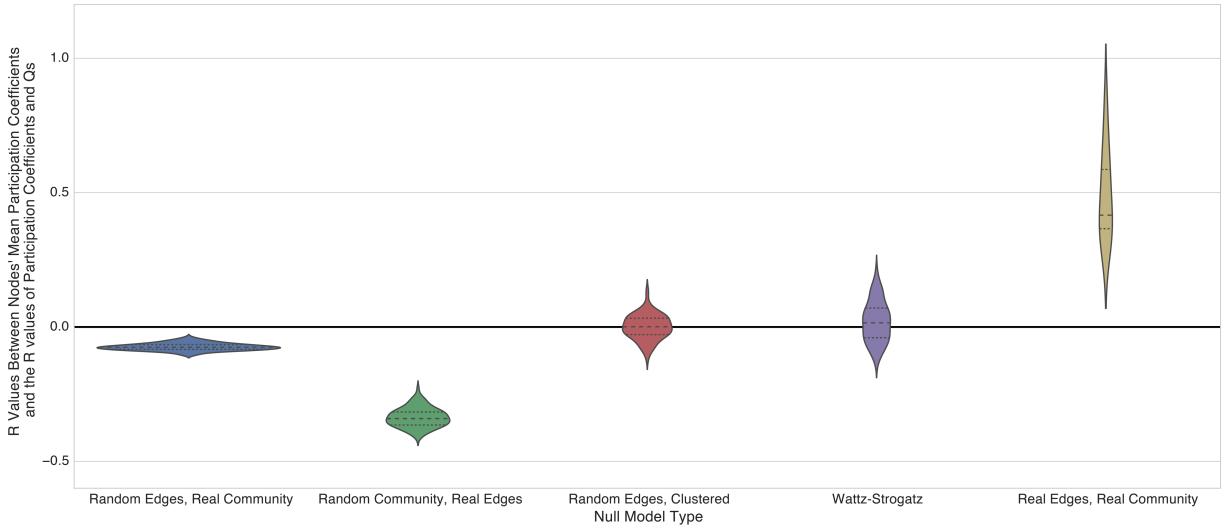

Supplementary Figure 8 | **Null Models**. We tested four null models of diversity facilitated modularity coefficients. (1) Random Edges, Real Community utilizes the true partition of nodes into communities that was uncovered by the application of community detection to each subject's intact resting-state graph (thresholded at a weighted graph density of 0.10, chosen based on this cost being the median cost from our original analyses), but we randomly permuted the edges uniformly after the partition was identified. (2) Random Community, Real Edges utilizes the partition of nodes into communities that was uncovered by the application of community detection to each subject's intact resting-state graph (thresholded at a weighted graph density of 0.10), but we then randomly permuted the assignment of nodes to communities (this retains the same number of communities and sizes of communities as the true partition). The edges remain in their true locations. (3) Random Edges, Clustered permutes the edges in each subject's resting-state graph uniformly at random. We then applied community detection to this permuted graph to identify a partition of nodes into communities, and then calculated the participation coefficient of each node based on that partition. We used a cost of 0.05, as denser random graphs result in just one community, which results in trivial participation coefficients of 0. For each instantiation (n=100) of each of these three models, we generated a graph for each subject using the subject's original graph and that particular null model. Finally, (4) we generated Wattz-Strogatz small world graphs. Each graph had 264 nodes with each node initially connected to its 7 neighbors in the lattice. We set the rewiring probability to 0.25. This results in Q values of roughly 0.40 and a binary density of roughly 0.05. 100 graphs were generated for each instantiation(n=100) of the model. For each null model, we then calculated the diversity facilitated modularity coefficient. Violin plots are shown for the distribution of the correlation between each node's mean participation coefficient and each node's diversity facilitated modularity coefficient across 100 instantiations of each model. For comparison, the distribution from the original analysis across tasks (Real Edges, Real Community) is also shown. N=264, the number of nodes in the graph, dof=262.

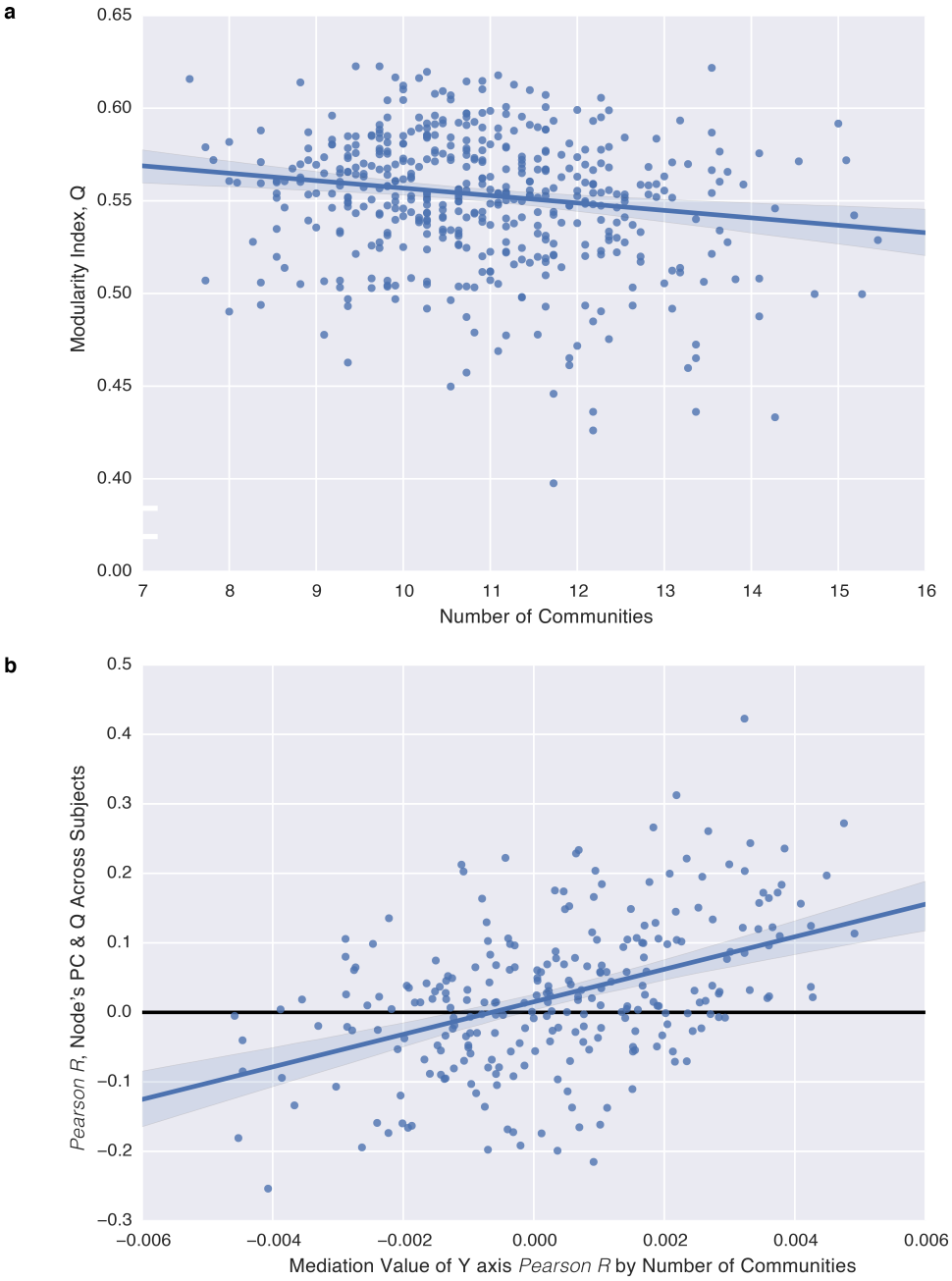

Supplementary Figure 9 | **Participation coefficients, the number of communities in the network, and modularity (*Q*)**. **a**, Negative correlation between the number of communities in subjects' graphs (averaged across graph densities in the range 0.05-0.15) and the *Q* value of the graphs (also averaged across graph densities in the range 0.05-0.15). **b**, We performed a mediation analysis between each node's participation coefficients, the number of communities in the graphs, and the *Q* values of the graphs, with the number of communities being the mediator. Mediation values are plotted for each node on the x-axis. The y-axis is the Pearson *r* between each node's participation coefficients and *Q* indices across subjects' graphs—the diversity facilitated modularity coefficient. Shaded areas represent a 95 percent confidence interval. *N*=264, the number of nodes in the graph, dof=262.

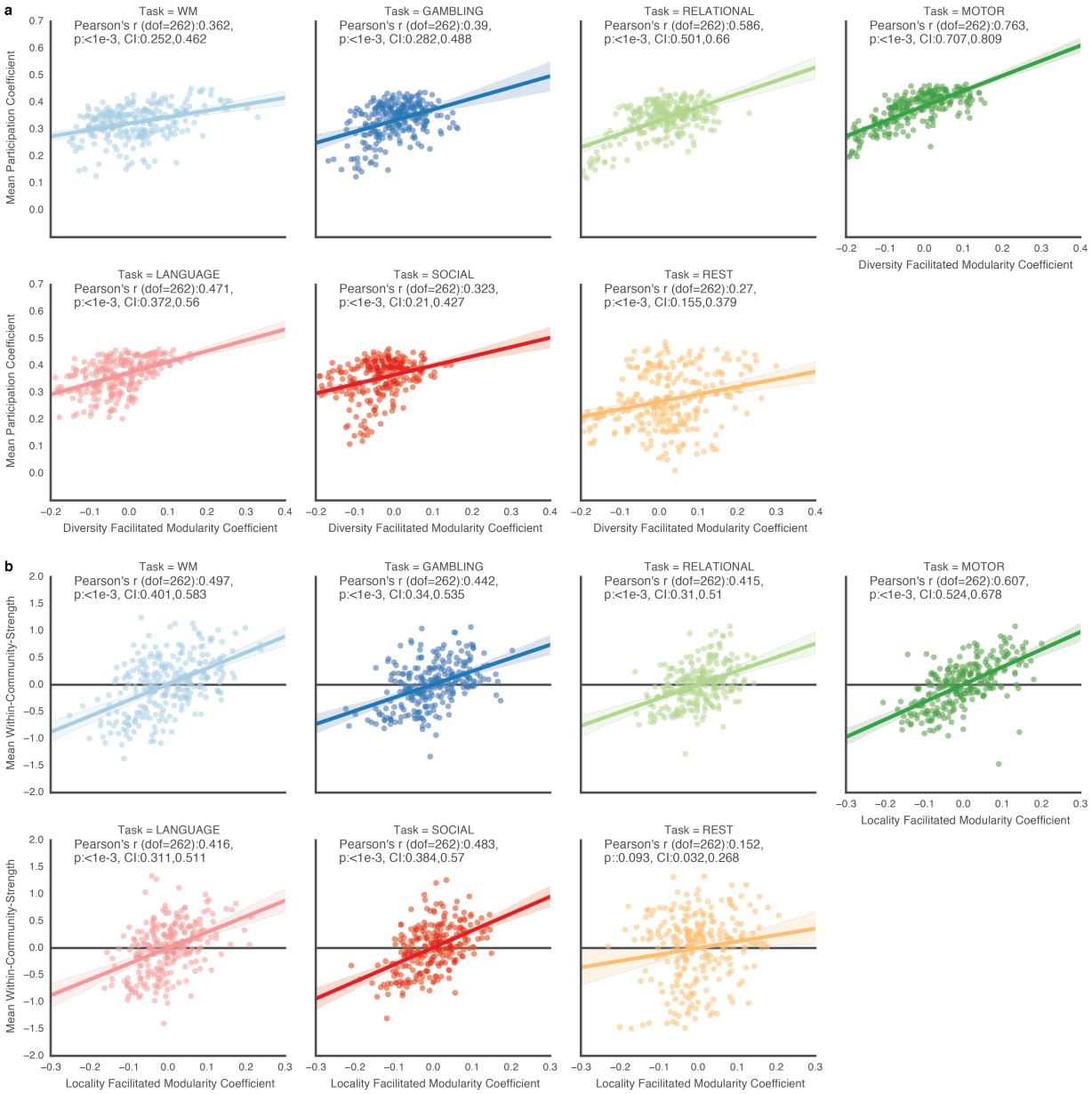

Supplementary Figure 10 | **Diversity and locality facilitated modularity coefficients controlling for the number of communities**. **a**, Correlations between a node's mean participation coefficient (across subjects) and the node's diversity facilitated modularity coefficient (the Pearson *r* correlation coefficient between that node's participation coefficients and modularity values (*Q*) across subjects after regressing out the number of communities in the network from *Q*). Correlations were calculated for each cognitive state. Each dot represents a node in the brain's functional network. Shaded areas represent 95 percent confidence intervals. In all cognitive states, there was a significant positive correlation between a node's mean participation coefficient and the node's diversity-facilitated modularity coefficient. **b**, Correlations between a node's mean within community strength (across subjects) and the node's locality facilitated modularity coefficient (Pearson *r* correlation coefficient between that node's within community strength and modularity values (*Q*) across subjects after regressing out the number of communities in the network from *Q*. In all cognitive states (except Resting state (uncorrected p=0.0132, Bonferroni corrected p=0.093), there was a significant positive correlation between a node's within community strength and the node's locality facilitated modularity coefficient. All *p* values are Bonferroni corrected (*n* tests=7). *N*=264, the number of nodes in the graph. *N* subjects=Working Memory:475, Gambling:473, Relational: 458, Motor:475, Language:472, Social: 474, Rest: 476.

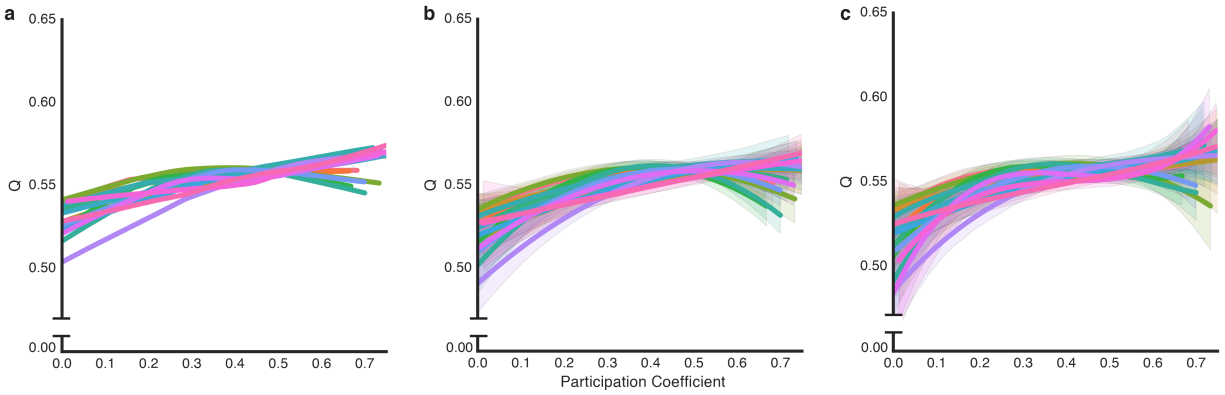

Supplementary Figure 11 | **Relationships between individual connector hubs' participation coefficients and *Q***. To test if the relationship between a connector hub's participation coefficients and *Q*—the connector hubs' diversity facilitated modularity coefficient—was linear, we fit three regression models to individual connector hubs' participation coefficients and *Q* values across subjects. In each plot, each line is the relationship between a single connector hub's participation coefficients and *Q* values across subjects. Only nodes with positive Pearson *r* values are shown. **a**, Locally weighted scatter-plot smoother fit. **b**, 2nd order fit. **c**, 3rd order fit. The relation between many connector hubs' participation coefficients and *Q* indices across subjects is well captured by a first order fit, with the hub's maximal participation coefficients (0.7; the mathematically upper limit is 0.9$\bar{9}$) corresponding to maximal *Q*. However, for example, some connector hubs' participation coefficients correspond to the maximal *Q* at a participation coefficient of 0.4-0.5, and then *Q* decreases at higher participation coefficients of that connector hub. Shaded areas represent 95 percent confidence intervals. *N*=476.

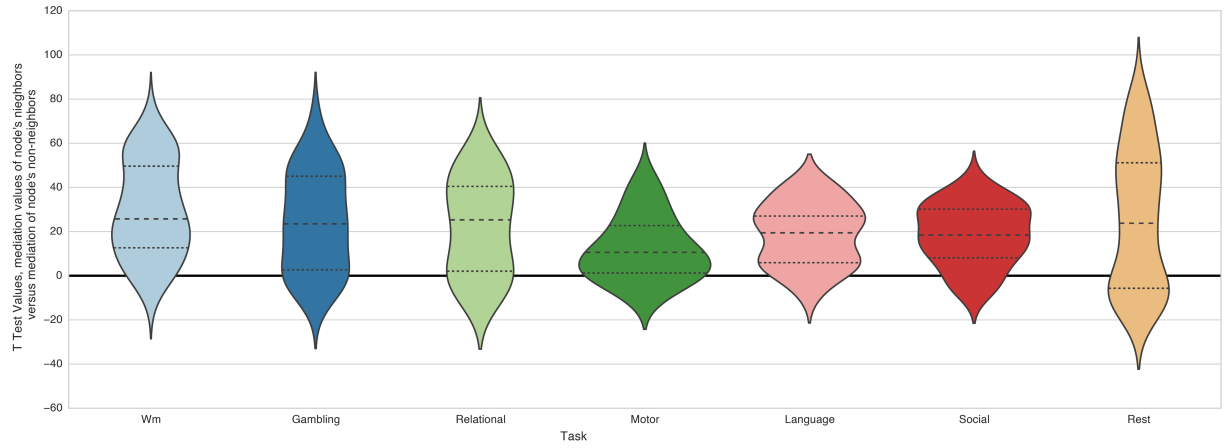

Supplementary Figure 12 | **Connector hubs' mediation of neighboring nodes' edges**. To investigate if the relationship between a connector hub's participation coefficient and *Q* is mediated primarily by that connector hub's neighbors' edge pattern increasing *Q* (per our prediction), we executed, for each connector hub node (*i*), a *t*-test between the absolute mediation values of node (*i*)'s neighbors' edges versus the absolute mediation values of node (*i*)'s non-neighbors' edges (neighbors were defined based on edges present between the two nodes in a graph at a density of 0.15, which was used because it is the densest density we utilized in our analyses; neighbors' and non-neighbors' edges connecting to the node (*i*) were ignored). Mediation values were based on the edge mediating between node (*i*)'s participation coefficients and modularity values *(Q)*; the distributions of mediation values was tested for normality using D'Agostino and Pearson's omnibus test k^2. All distributions were confirmed as normal (k^2>100.0, $p<0.001$ for all tasks). The distribution of *t*-values for connector hubs is shown for each task. The mean quartiles are marked. In general, connector hubs showed higher mediation values with edges of its neighbors compared to the edges of its non-neighbors (i.e., *t*>0). Moreover, these *t*-values were significantly higher than the same *t*-values calculated with local hubs (*t*(dof:1358): 3.892, *p*:0.0001, Cohen's *d*:0.219, CI:1.887,6.62).

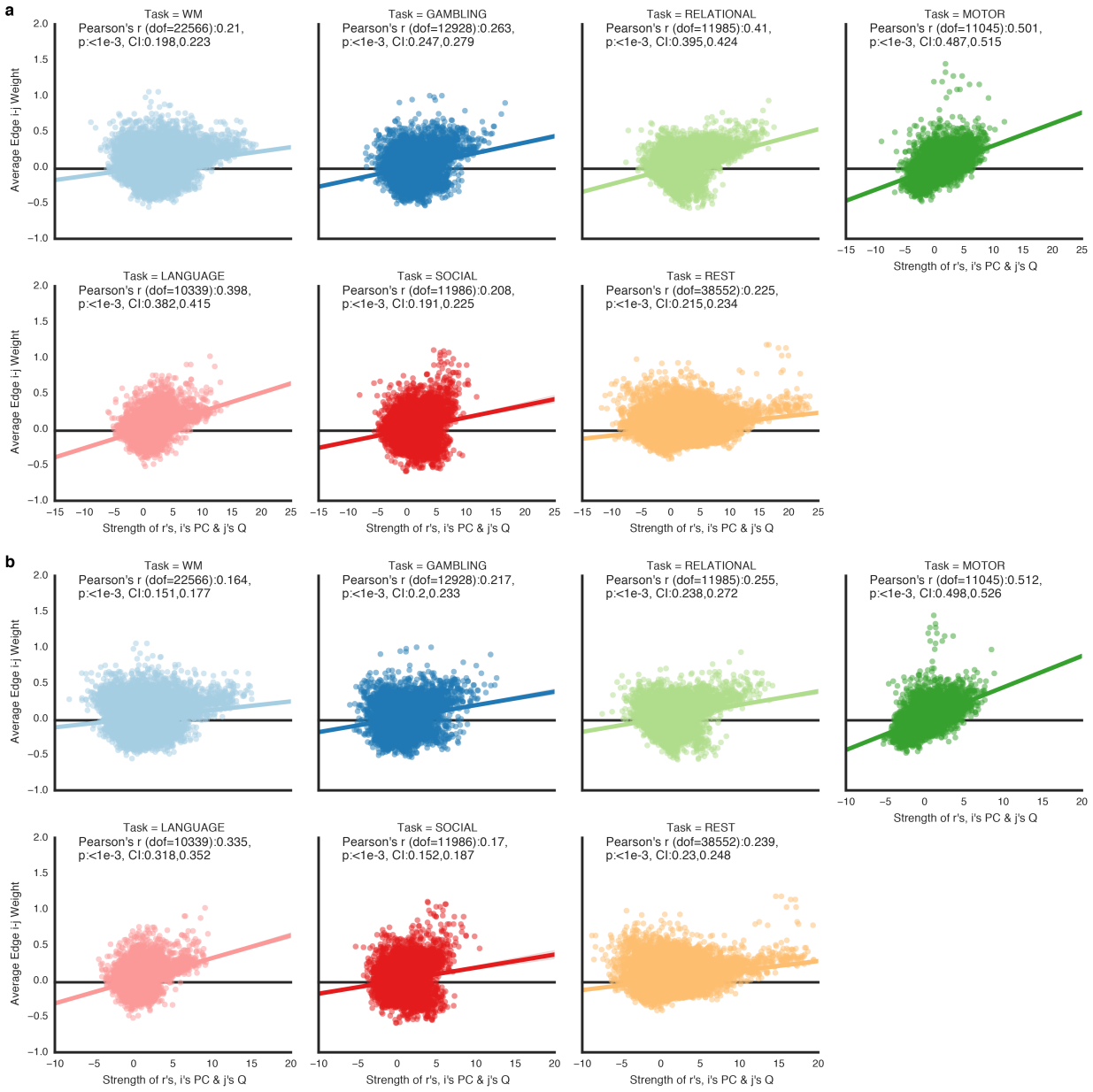

Supplementary Figure 13 | **Connector hubs' relationships with individual edges' weights**. **a**,**b**, For each task, for each pair of nodes *i* and *j*, we calculated the correlation between (*x*) how strongly node *i* increased the within community edge strength of node *j* (the sum of Pearson *r* values between the participation coefficients of node *i* and the within community edges of node *j* minus the sum of Pearson r values between the participation coefficients of node *i* and the between community edges of node *j*) with (y) the average connectivity edge weight between node *i* and node *j*. **a** Includes all positive edges, while **b** includes the strongest 25 percent of edges. Bonferroni corrected *p* values are shown in all plots (*n* tests = 7). These results show that connector hubs are predominately tuning the connectivity of their neighbors. Shaded areas represent 95 percent confidence intervals. *N*=dof+2 for each panel.

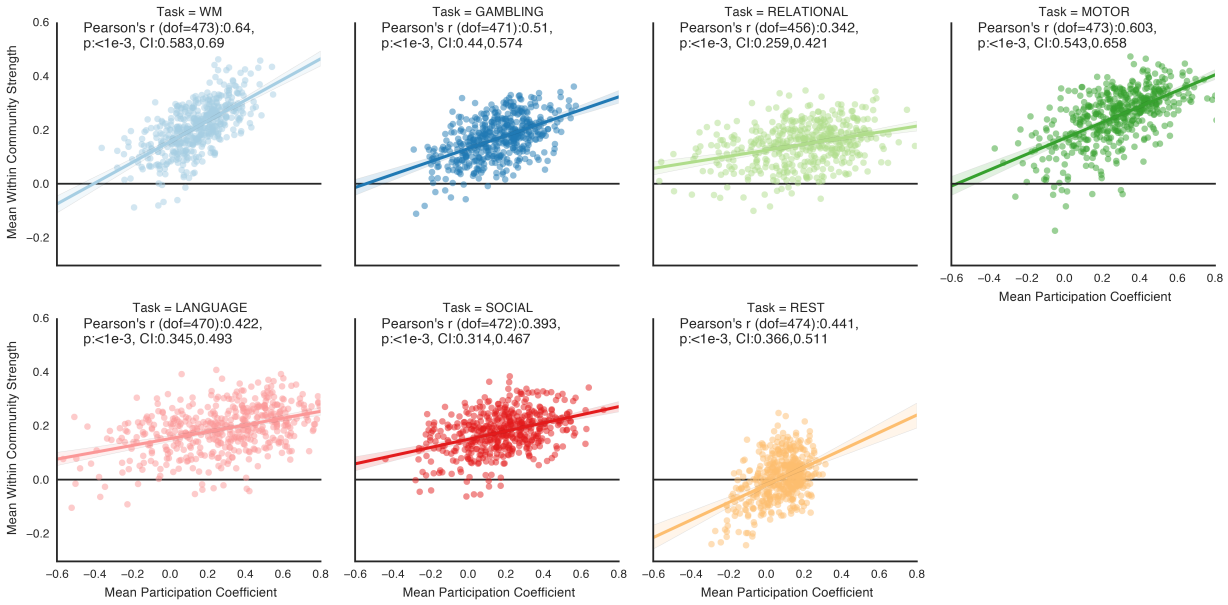

Supplementary Figure 14 | **Connector hubs and local hubs are interrelated**. For each task, across subjects, the correlation between the subject's connector hubs' mean participation coefficient and the subject's local hubs' mean within community strengths. In every task, if a subject's connector hubs were diverse, local hubs were local. Here, connector and local hubs were defined based on nodes for which their diversity and locality (respectively) facilitated modularity coefficients were positive. For this calculation, participation coefficients were z-scored within each subject, as within community strengths are z-scored within each subject. Bonferroni corrected *p* values are reported in all plots(*n* tests = 7). Shaded areas represent 95 percent confidence intervals. *N*=Working Memory:475, Gambling:473, Relational: 458, Motor:475, Language:472, Social: 474, Rest: 476.

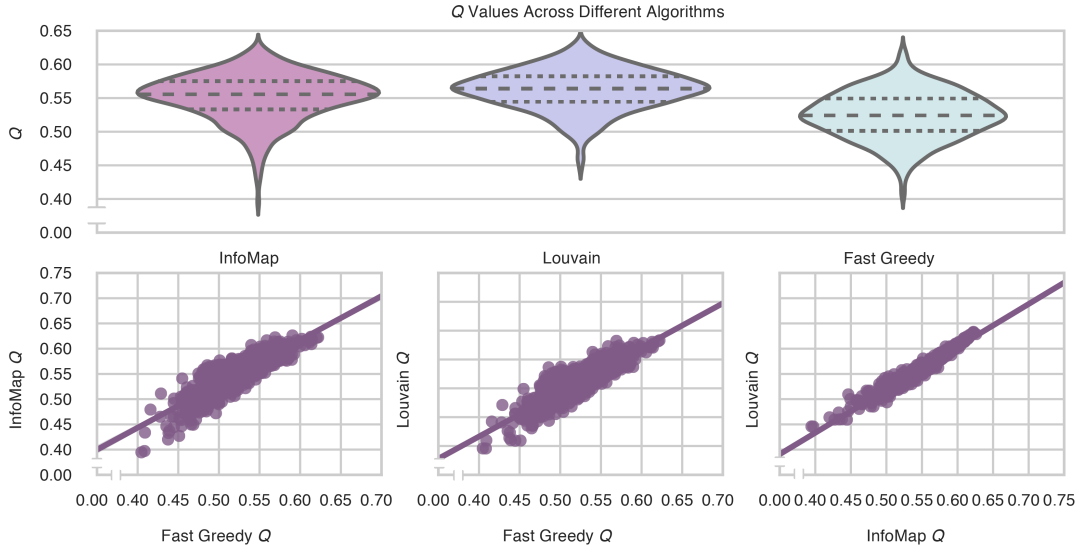

Supplementary Figure 15 | **Modularity quality indices from three community detection algorithms**. We used *Q* indices repeatedly in our analyses. However, the community detection algorithm that we utilized, InfoMap, does not explicitly maximize *Q*. To see if this could potentially impact our analyses, we compared *Q* values from InfoMap to two popular algorithms, Fast-Greedy and Louvain, that explicitly maximize *Q*. The mean *Q* value, as in our analyses, was taken across costs of 0.05 to 0.15. **a**, Distribution, across subjects, of *Q* values of each algorithm. **b**, Correlation between Q values across algorithms. Shaded areas represent 95 percent confidence intervals. In all panels, *N*=476, dof=474.